

**SYNTHESIS AND CHARACTERISATION OF  
MICROPOROUS AIPO-5 MOLECULAR SIEVES  
TEMPLATED BY NOVEL IMIDAZOLIUM-BASED  
STRUCTURAL DIRECTING AGENTS**

by

**DAMIEN KHOO YIYUAN**

**Thesis submitted in fulfillment of the requirements**

**for the degree of**

**Master of Science**

**August 2013**

## ACKNOWLEDGEMENT

First and foremost, I would like extend my sincere token of gratitude to my supervisor, Dr. Ng Eng Poh for his continuous guidance, motivation patience and support throughout my course of study. I would also like to acknowledge Universiti Sains Malaysia (USM) and School of Chemical Sciences for the facilities and support provided in making this study a success.

I would also take this opportunity to thank the Ministry of Higher Education of Malaysia (MOHE) for providing me with a scholarship under the MyBrain 15-MyMaster Programme. Thanks to the Institute of Postgraduate Studies (IPS) for providing me financial assistance through the Graduate Assistant Scheme.

This study is made possible thanks to the Research Creativity and Management Office (RCMO) for the RU-PGRS grant (101/PKIMIA/835009) and USM Short-Term Grant (304/PKIMIA/6310084) and COMSTECH-TWAS for their research grants.

Special thanks to all the academic and non-academic staff of School of Chemical Sciences for their assistant over the course of this study. I am grateful to the School of Biological Sciences, School of Physics, Professor Svetlana Mintova from Université de Caen, France and Dr. Rino R. Mukti from Institut Teknologi Bandung, Indonesia for their assistance in conducting SEM, XRD and N<sub>2</sub> adsorption analyses. I am grateful to all members of my group for brightening up the lab and their support during the day to day running of my research project.

This thesis is dedicated to my parents. Without their love, patience, encouragement and support, my master degree would have been a lot harder and less enjoyable. Thanks for putting up with me through the stressful times and always believing in me.

**Damien Khoo Yiyuan**

**August 2013**

## TABLE OF CONTENTS

	Page
ACKNOWLEDGEMENTS	ii
TABLE OF CONTENTS	iv
LIST OF ABBREVIATIONS	ix
LIST OF TABLES	xi
LIST OF SCHEMES	xii
LIST OF FIGURES	xiii
LIST OF APPENDICES	xviii
ABSTRAK	xix
ABSTRACT	xxi

### CHAPTER 1: INTRODUCTION

1.1	General introduction	1
1.2	Objectives of study	2
1.3	Scope of thesis	2

### CHAPTER 2: LITERATURE REVIEW

2.1	Porous materials	5
2.1.1	Microporous materials	6
2.2	Zeolite and aluminophosphate (AIPO) materials	7
2.2.1	Zeolite materials	7
2.2.2	Aluminophosphate (AIPO) materials	9
2.2.3	Comparison between zeolite and AIPO materials	11

2.2.4	Nomenclature, structure building unit (SBU) and framework structure of AlPO materials	13
2.3	Hydrothermal synthesis of AlPO materials	16
2.3.1	Structure-directing agent	18
2.3.2	Mechanism of crystallisation	21
2.3.2.1	Solution-mediated transport mechanism	24
2.3.2.2	Solid hydrogel transformation mechanism	24
2.3.2.3	Autocatalytic nucleation mechanism	26
2.4	Ionothermal synthesis of AlPO materials	27
2.4.1	Ionic liquid	27
2.4.2	Synthesis	29
2.5	Porosity of AlPO materials	31
2.5.1	Removal of organic SDAs from AlPO micropores	31
2.5.2	AlPO-5 molecular sieves in dye removal	33

### **CHAPTER 3: EXPERIMENTAL METHODOLOGY**

3.1	Overview	34
3.2	Ionothermal synthesis of AlPO-5 molecular sieves	
3.2.1	Synthesis of 1-ethyl-2,3-dimethylimidazolium bromide, [edmim]Br ionic molten salt, <b>I</b>	36
3.2.2	Synthesis of AlPO-5 molecular sieve	37
3.3	Hydrothermal synthesis of AlPO-5 molecular sieves	
3.3.1	Synthesis of 2,3-O-isopropylidene-1-O-p-tolyl-sulfonylglycerol (tosylate ester), <b>II</b>	39

3.3.2	Synthesis of 3-(2,3-dihydroxypropyl)-1,2-dimethylimidazolium-4-methylbenzenesulfonate, <b>III</b>	40
3.3.3	Synthesis of 3-(2,3-dihydroxypropyl)-1,2-dimethylimidazolium hydroxide, [dhpdm]OH, <b>IV</b>	40
3.3.4	Synthesis of AlPO-5 molecular sieves	42
3.3.5	Template removal of organic template	44
3.3.5.1	Calcination	44
3.3.5.2	Microwave-assisted Fenton-liked oxidation	44
3.3.6	Adsorption study of AlPO-5 molecular sieves	45
3.4	Characterisation techniques	46
3.4.1	Fourier transformed infrared (FT-IR) spectroscopy	46
3.4.2	$^1\text{H}$ and $^{13}\text{C}$ NMR spectroscopy	46
3.4.3	Elemental CHNSO analysis	47
3.4.4	Powder X-ray diffraction (XRD) analysis	47
3.4.5	Field emission scanning electron microscopy (FESEM)	47
3.4.6	$^{27}\text{Al}$ and $^{31}\text{P}$ solid-state CP MAS NMR spectroscopy	47
3.4.7	Thermogravimetric and differential thermal analysis (TG/DTA)	48
3.4.8	$\text{N}_2$ adsorption analysis	48
3.4.9	Ultra-violet visible (UV-Vis) spectrophotometry	48

## CHAPTER 4: RESULTS AND DISCUSSION

4.1	Overview	49
4.2	Ionothermal synthesis of AlPO-5 molecular sieves	50
4.2.1	Evolution and crystallisation process of AlPO-5	50

4.2.2	Confinement study of [edmim]Br in AlPO-5 crystals	55
4.2.3	Local environment of AlPO-5 crystals	58
4.2.4	TG/DTA analysis	60
4.2.5	Effects of synthesis parameters	63
4.2.5.1	Effect of [edmim]Br content	63
4.2.5.2	Effect of Al <sub>2</sub> O <sub>3</sub> /P <sub>2</sub> O <sub>5</sub> molar ratio	66
4.2.5.3	Effect of H <sub>2</sub> O content	68
4.3	Hydrothermal synthesis of AlPO-5 molecular sieves	70
4.3.1	Effects of synthesis parameters	70
4.3.1.1	Effect of crystallisation time	70
4.3.1.2	Effect of [dhpdm]OH content	75
4.3.1.3	Effect of H <sub>2</sub> O content	78
4.3.1.4	Effect of Al <sub>2</sub> O <sub>3</sub> /P <sub>2</sub> O <sub>5</sub> molar ratio	81
4.3.1.5	Effect of synthesis temperature	83
4.3.2	Structural investigation of AlPO-5 <i>via</i> <sup>27</sup> Al and <sup>31</sup> P solid-state CP MAS NMR	86
4.3.3	Supramolecular study of [dhpdm]OH in AlPO-5 crystals	89
4.3.4	TG/DTA analysis	91
4.3.5	[dhpdm]OH detemplating study	94
4.3.6	Study of N <sub>2</sub> adsorption isotherm analysis	99
4.3.7	Adsorption of methylene blue study	101

## CHAPTER 5: CONCLUSION

5.1	Thesis summary	103
5.2	Recommendations for future works	105

REFERENCES	106
APPENDICES	114
LIST OF PUBLICATIONS	119



## LIST OF SYMBOLS, ABBREVIATIONS AND NOMENCLATURES

Abbreviations/ symbols	Descriptions
AFI	Aluminophosphate-5
[bmim]OH	1-Butyl-3-methylimidazolium hydroxide
[dhpdm]OH	3-(2,3-Dihydroxylpropyl)-1,2-dimethylimidazolium hydroxide
[edim]Br	1-Ethyl-2,3-dimethylimidazolium bromide
[emim]OH	1-Ethyl-3-methylimidazolium hydroxide
$^{13}\text{C}$ NMR	Carbon-13 nuclear magnetic resonance
$^1\text{H}$ NMR	Proton nuclear magnetic resonance
AlPO	Aluminophosphate
BET	Brunauer-Emmet-Teller
CP/MAS	Cross-polarization magic angle spinning
DMSO	Dimethyl sulphoxide
D <sub>2</sub> O	Deuterium oxide
FESEM	Field emission scanning electron microscopy
FTIR	Fourier transform infrared
IL	Ionic liquid
MB	Methylene blue
NMR	Nuclear magnetic resonance
$S_{\text{BET}}$	Specific BET surface area
SDA	Structure-directing agent
$S_{\text{micropore}}$	Micropore surface area
TBAOH	Tetrabutylammonium hydroxide

<b>Abbreviations/ symbols</b>	<b>Descriptions</b>
TEA	Tetraethylamine
TEAOH	Tetraethylammonium hydroxide
TG/DTA	Thermogravimetric and differential thermal analysis
TPA	Tetrapropylamine
TPAOH	Tetrapropylammonium hydroxide
UV-Vis	Ultraviolet-visible
$V_{\text{total}}$	Total pore volume
XRD	X-ray diffraction

## LIST OF TABLES

	Page
Table 2.1    Structure framework and pore size of several AlPO materials[23].	10
Table 2.2    Comparison of properties between AlPO and zeolite molecular sieves.	12
Table 3.1    Ionothermal synthesis conditions and phase of the obtained products.	38
Table 3.2    Hydrothermal synthesis conditions and phase of the obtained products.	43
Table 4.1    Properties of AlPO-5 products obtained <i>via</i> ionothermal synthesis.	54
Table 4.2    Properties of AlPO-5 products obtained <i>via</i> hydrothermal synthesis.	73
Table 4.3    Physico-chemical properties of Fenton-oxidised HS-12 and calcined HS-12 samples.	100

## LIST OF SCHEMES

	Page
Scheme 2.1 Schematic equations for Fenton-liked oxidation process.	33
Scheme 3.1 Synthesis route for compound I.	36
Scheme 3.2 Synthesis route for compounds II, III and IV.	41

## LIST OF FIGURES

		Page
Figure 2.1	Schematic representation of the classification of nanoporous materials[2].	6
Figure 2.2	(a) Zeolite framework with alternating $\text{AlO}_4^-$ and $\text{SiO}_4$ tetrahedra and (b) AlPO framework with alternating $\text{AlO}_4^-$ and $\text{PO}_4^+$ tetrahedra.	8
Figure 2.3	Secondary building units (SBUs) found in nanoporous materials which contain $\text{TO}_4$ tetrahedra[13].	15
Figure 2.4	Illustration of AlPO-5 structure with AFI framework formed by arrangement of separate cages[21].	15
Figure 2.5	Schematic illustration of the hydrothermal synthesis of AlPO materials.	18
Figure 2.6	Process of crystal growth in solution.	21
Figure 2.7	Schematic representation of the three-stage AlPO-5 crystallisation[43].	23

Figure 2.8	(a) Schematic illustration of the solution-mediated transport mechanism involving the diffusion of ionic aluminate, silicate/phosphate species from the liquid phase to the nucleation site for crystal growth[44], and (b) Schematic illustration of the solid hydrogel transformation mechanism involving the reorganization of the solid hydrogel to form the molecular sieve structure[15].	25
Figure 2.9	Examples of cations used in ionic liquids.	28
Figure 2.10	Examples of anions used in ionic liquids.	29
Figure 3.1	Schematic flow of experimental methodology for (a) hydrothermal and (b) ionothermal studies.	35
Figure 4.1	XRD diffractograms and SEM images (inset) of (a) IT-1 ( $t = 20$ h), (b) IT-2 ( $t = 44$ h), (c) IT-3 ( $t = 90$ h) and (d) IT-5 ( $t = 140$ h) with different crystallisation times. The solid products were obtained with a molar composition of $1\text{Al}_2\text{O}_3$ : $75[\text{edmim}]\text{Br}$ : $1.8\text{P}_2\text{O}_5$ : $3.5\text{H}_2\text{O}$ , $150^\circ\text{C}$ .	52
Figure 4.2	FT-IR spectra of (a) [edmim]Br ionic liquid and (b) fully crystalline AlPO-5 (IT-3) solids.	57
Figure 4.3	(a) $^{27}\text{Al}$ and (b) $^{31}\text{P}$ CP MAS NMR spectra of micro crystalline AlPO-5 solid (IT-3). Asterisks denote spinning bands.	59

Figure 4.4	TGA/DTA thermograms of (a) pure [edmim]Br ionic liquid and (b) as-synthesised AlPO-5 (IT-3) solid.	62
Figure 4.5	XRD diffractograms and SEM images (inset) of (a) IT-9 ( $x = 150$ ), (b) IT-8 ( $x = 100$ ), (c) IT-7 ( $x = 75$ ) and (d) IT-6 ( $x = 50$ ) with different [edmim]Br molar ratio. The solid products were obtained with a molar composition of $1\text{Al}_2\text{O}_3: x[\text{edmim}]\text{Br}: 2.84\text{P}_2\text{O}_5: 5.46\text{H}_2\text{O}$ , $150\text{ }^\circ\text{C}$ , 90 h.	65
Figure 4.6	XRD diffractograms and SEM images (inset) of (a) IT-10 ( $y = 0.8$ ), (b) IT-11 ( $y = 1.4$ ), (c) IT-12 ( $y = 2.4$ ) and (d) IT-14 ( $y = 3.8$ ) with different $\text{P}_2\text{O}_5/\text{Al}_2\text{O}_3$ molar ratios. The solid products were obtained with a molar composition of $1\text{Al}_2\text{O}_3: 75[\text{edmim}]\text{Br}: y\text{P}_2\text{O}_5: 3.5\text{H}_2\text{O}$ , $150\text{ }^\circ\text{C}$ , 90 h.	67
Figure 4.7	XRD diffractograms and SEM images (inset) of (a) IT-15 ( $z = 1$ ), (b) IT-16 ( $z = 5.5$ ) and (c) IT-17 ( $z = 15.0$ ) with different $\text{H}_2\text{O}$ molar ratios. The solid products were obtained with a molar composition of $1\text{Al}_2\text{O}_3: 100[\text{edmim}]\text{Br}: 2.84\text{P}_2\text{O}_5: z\text{H}_2\text{O}$ , $150\text{ }^\circ\text{C}$ , 90 h.	69
Figure 4.8	XRD patterns of (a) HS-1 ( $t = 4\text{ h}$ ), (b) HS-2 ( $t = 6\text{ h}$ ), (c) HS-3 ( $t = 8\text{ h}$ ) and (d) HS-4 ( $t = 15\text{ h}$ ) with different period of crystallisation. The solid products were obtained with a molar composition of $1\text{Al}_2\text{O}_3: 3.0[\text{dhpdm}]\text{OH}: 2.5\text{P}_2\text{O}_5: 80\text{H}_2\text{O}$ , $180\text{ }^\circ\text{C}$ .	72
Figure 4.9	SEM images of (a) HS-3, (b) HS-6, (c) HS-9 and (d) HS-12 exhibiting different morphologies.	74

Figure 4.10	XRD diffractograms (a) HS-5 ( $x = 1.0$ ), (b) HS-3 ( $x = 3.0$ ), (c) HS-6 ( $x = 4.0$ ) and (d) HS-7 ( $x = 5.0$ ) with different [dhpdm]OH molar ratios. The solid products were obtained with a molar composition of $1\text{Al}_2\text{O}_3$ : $x[\text{dhpdm}]\text{OH}$ : $2.5\text{P}_2\text{O}_5$ : $80\text{H}_2\text{O}$ , $180\text{ }^\circ\text{C}$ , 8 h.	77
Figure 4.11	XRD diffractograms of (a) HS-8 ( $y = 40$ ), (b) HS-9 ( $y = 60$ ), (c) HS-3 ( $y = 80$ ) and (d) HS-10 ( $y = 120$ ) with different water contents. The solid products were obtained with a molar composition of $1\text{Al}_2\text{O}_3$ : $3.0[\text{dhpdm}]\text{OH}$ : $2.5\text{P}_2\text{O}_5$ : $y\text{H}_2\text{O}$ , $180\text{ }^\circ\text{C}$ , 8 h.	80
Figure 4.12	XRD patterns of (a) HS-11 ( $z = 0.5$ ), (b) HS-12 ( $z = 1.1$ ), (c) HS-3 ( $z = 2.5$ ) and (d) HS-13 ( $z = 3.0$ ) with different $\text{P}_2\text{O}_5/\text{Al}_2\text{O}_3$ molar ratios. The solid products were obtained with a molar composition of $1\text{Al}_2\text{O}_3$ : $3.0[\text{dhpdm}]\text{OH}$ : $z\text{P}_2\text{O}_5$ : $80\text{H}_2\text{O}$ , $180\text{ }^\circ\text{C}$ , 8 h. Asterisks denote presence of impurity phase.	82
Figure 4.13	XRD patterns of (a) HS-15 ( $t = 8$ ), (b) HS-16 ( $t = 14$ ), (c) HS-17 ( $t = 22$ ) and (d) HS-18 ( $t = 32$ ). The HS-15 and HS-16 solid products were obtained with a molar composition of $1\text{Al}_2\text{O}_3$ : $4.0[\text{dhpdm}]\text{OH}$ : $2.5\text{P}_2\text{O}_5$ : $80\text{H}_2\text{O}$ , $160\text{ }^\circ\text{C}$ , $t$ h while HS-17 and HS-18 solid products were obtained with a molar composition of $\text{Al}_2\text{O}_3$ : $3.0[\text{dhpdm}]\text{OH}$ : $1.1\text{P}_2\text{O}_5$ : $80\text{H}_2\text{O}$ , $140\text{ }^\circ\text{C}$ , $t$ h. Asterisks denote presence of AlPO-5 phase.	85
Figure 4.14	Illustration of AlPO-5 framework structure indicating the local environment for the Al and P species.	86
Figure 4.15	(a) $^{27}\text{Al}$ and (b) $^{31}\text{P}$ CP MAS NMR spectra of micro-crystalline AlPO-5 solid (HS-12).	88
Figure 4.16	FT-IR spectra of (a) [dhpdm]OH organic template and (b) fully crystalline AlPO-5 (HS-12) solids.	90



Figure 4.17	TGA/DTA thermograms of (a) [dhpdm]OH organic template and (b) as-synthesised AlPO-5 (HS-12) solid.	93
Figure 4.18	FT-IR spectra and physical appearance of HS-12 solid (a) before calcination and after calcination at (b) 500 °C, (c) 600 °C and (d) 700 °C.	97
Figure 4.19	FT-IR spectra and physical appearance of AlPO-5 solid (HS-12) (a) before, (b) after microwave-assisted Fenton-like oxidation and (c) after calcination at 700 °C.	97
Figure 4.20	XRD diffractograms of HS-12 solid (a) before, (b) after calcination at 700 °C and (c) after microwave-assisted Fenton-like oxidation.	99
Figure 4.21	Nitrogen gas adsorption isotherms of HS-12 solid after (a) microwave-assisted Fenton-like oxidation and (b) calcination at 700 °C. Closed symbols represent adsorption and open symbols represent desorption.	100
Figure 4.22	Effect of solution temperature on MB adsorption on (a, c) Fenton-oxidized AlPO-5 sample and (b, d) calcined AlPO-5 samples.	102

## LIST OF APPENDICES

	Page
Appendix-1 $^1\text{H}$ NMR spectrum of [edmim]Br.	114
Appendix-2 $^1\text{H}$ NMR spectrum of [dhpdm]OH.	115
Appendix-3 $^{13}\text{C}$ NMR spectrum of [dhpdm]OH.	116
Appendix-4 Photographs of methylene blue solution after calcined HS-12 AlPO-5 treatment at 30 °C.	117
Appendix-5 Photographs of methylene blue solution after calcined HS-12 AlPO-5 treatment at 50 °C.	117
Appendix-6 Photographs of methylene blue solution after Fenton-oxidised HS-12 AlPO-5 treatment at 30 °C.	118
Appendix-7 Photographs of methylene blue solution after Fenton-oxidised HS-12 AlPO-5 treatment at 50 °C.	118

**SINTESIS DAN PENCIRIAN PENAPIS MOLEKUL MIKROLIANG AIPO-5  
YANG DIACUANKAN OLEH AGEN PENGSTRUKTURAN BARU  
BERASASKAN IMIDAZOLIUM**

**ABSTRAK**

Penapis molekul mikroliang aluminolfosfat (AIPO) telah disintesis melalui kaedah hidroterma dan kaedah ionoterma. Sintesis melalui kaedah hidroterma menggunakan 3-2(2,3-dimetilimidazolium hidroksida), [dhpdm]OH, sebagai suatu agen pengstruktur (SDA) baru sementara kaedah ionoterma dijalankan dengan menggunakan 1-etil-2,3-dimetilimidazolium bromida, [edmim]Br, cecair ionik sebagai agen pengarah dan pelarut. Kedua-dua kaedah ini dikaji dengan mengoptimakan keadaan sintesis iaitu suhu dan tempoh sintesis dan kepekatan molar SDA, nisbah  $P_2O_5/Al_2O_3$  dan  $H_2O$  dalam gel sintesis. Hasil kajian mendapati pelbagai morfologi hablur AIPO-5(AFI) yang memiliki topologi AFI diperoleh hasil daripada penggunaan keadaan sintesis yang berbeza. Kaedah sintesis hidroterma yang menggunakan [dhpdm]OH telah menghasilkan hablur yang berbentuk turus jalur, gumpalan prisma heksagon, setong heksagon dan rod silinder. Di samping itu, sintesis melalui kaedah ionoterma menggunakan [edmim]Br pula menghasilkan gumpalan hablur berbentuk kepingan heksagon dan hablur bijian yang berbentuk heksagon.

Kajian terhadap [dhpdm]OH dan [edmim]OH yang terkurung di dalam mikroliang AIPO-5 dijalankan dengan kaedah spektroskopi FT-IR dan analisis TG/DTA. Molekul [dhpdm]OH didapati berinteraksi kuat dengan rangka AIPO-5 dan menyebabkan molekul organik tersebut hanya dapat dikeluarkan daripada mikroliang AIPO-5 pada suhu yang lebih tinggi berbanding dengan [edmim]Br. Bagi

mengaplikasikan penapis molekul mikroliang AIPO-5, molekul organik di dalam mikroliang AIPO-5 dikeluarkan untuk menghasilkan bahan yang berliang. Molekul organik, [dhpdm]OH, dikeluarkan melalui kaedah pengkalsinan AIPO-5 pada suhu yang tinggi dan kaedah pengoksidaan Fenton. Kaedah kedua didapati lebih menjimatkan tenaga dan merupakan kaedah yang lebih berkesan untuk mengeluarkan molekul organik [dhpdm]OH.

Cubaan untuk menggunakan penapis molekul mikroliang AIPO-5 tersebut untuk menjerap pewarna larutan metilena biru telah dijalankan. Kajian tersebut mendapati bahawa AIPO-5 dapat menyingkirkan 16% metilena biru.

**SYNTHESIS AND CHARACTERISATION OF MICROPOROUS AIPO-5  
MOLECULAR SIEVES TEMPLATED BY NOVEL IMIDAZOLIUM-BASED  
STRUCTURAL DIRECTING AGENTS**

**ABSTRACT**

Microporous aluminophosphate (AIPO) molecular sieves have been successfully crystallised under hydrothermal and ionothermal syntheses. The former approach engaged 3-(2,3-dihydroxypropyl)-1,2-dimethylimidazolium hydroxide, [dhpdm]OH, as a new structure-directing agent (SDA). The ionothermal synthesis was carried out by using 1-ethyl-2,3-dimethylimidazolium bromide, [edmim]Br ionic liquid, as both solvent and structure-directing agent. Both methods were investigated by optimising the synthesis conditions such as crystallisation time and temperature and molar concentrations of SDA,  $P_2O_5/Al_2O_3$  ratio and  $H_2O$  in precursor gels. The results obtained showed different morphologies of well-defined AIPO-5 (AFI) crystals with AFI topology under different synthesis conditions. Hydrothermal treatment using [dhpdm]OH produced crystals with column-strip, aggregated hexagonal prism, hexagonal barrel and narrow cylindrical rod structures. On the other hand, ionothermal treatment using [edmim]Br ionic liquid yielded aggregated and spheroidal hexagonal thin-plate crystals.

Supramolecular study of [dhpdm]OH and [edmim]Br molecules in the AIPO-5 microporous materials are conducted using FT-IR spectroscopy and TG/DTA analysis. The [dhpdm]OH molecules were found to have very strong interaction with the AIPO-5 framework as these molecules could only be removed from the AIPO-5 micropores at a higher temperature compared to the case of [edmim]Br. In order for

the AlPO-5 to be used for further purposes, the SDA was removed from the pore cavity of the AlPO-5 framework to create microporous void space. Porous AlPO-5 in this study was prepared from a selected hydrothermal-treated AlPO-5 molecular sieve by calcination which required a high temperature and a combustion-free method known as Fenton-liked oxidation process. It was found that the more energy-saving Fenton-liked oxidation method was a more effective technique to remove [dhpdm]OH organic template.

The synthesised porous AlPO-5 molecular was used to remove dye pollutants. The synthesised AlPO-5 molecular sieves were able to remove 16% methylene blue dye solution.

## **CHAPTER 1**

### **INTRODUCTION**

#### **1.1. General introduction**

With the rapid advancement and development of nanotechnology, the emergence of nanosized materials in the market has received tremendous demands from industries of various fields. Addressing to the needs of today's market, extensive research has been mobilised to produce scalable and economical nanomaterials; one of which zeolitic materials. Zeolites and zeotypes molecular sieves are groups of microporous minerals which have been widely used in a variety of industrial applications such as catalysts in the oil refining and petrochemical industry, as ion-exchange beds in domestic and commercial water purification as well as in gas separation, as adsorbents in wastes treatment industry, and as hosts for drug delivery system in biochemical and biomedical industry. Over the decades, these aforementioned materials are produced hydrothermally and ionothermally (most recent approach), but with the lack of a full understanding to the formation mechanism for these materials. Though the recipes to prepare these materials are found empirically, it is still not possible to intentionally create new framework.

It is hypothesised that, the nucleation and growth process of these microporous materials depend on the solvent and structure-directing agent participated in the process. The flexibility and rigidity of the structure-directing agents influence the framework structures to which the zeolitic materials adapt. The confirmation of the organic template must be able to direct the precursors into forming a specific

framework and fits well in order to stabilise the achieved framework. Therefore, it is very crucial to find a suitable organic template to selectively-direct the crystallisation of the aforementioned microporous materials.

### **1.2. Objectives of study**

This study was carried out to explore new alternative approaches to synthesis microporous AlPO materials through a self-prepared novel imidazolium-based SDA which contains a diol functional group. Thus, two organic SDAs were utilised in the synthesis of AlPO materials *via* the hydrothermal and ionothermal methods. This study was aimed to investigate the morphological versatility of AlPO materials through optimisation of different synthesis conditions such as heating time and concentrations of precursors and SDA. Conventional organic template removal method *via* calcination method requires a lot of energy, thus making it less environmental friendly. This study aimed to propose the microwave-assisted Fenton-like oxidation process as a organic template removal method which requires less energy and the method is time-saving.

### **1.3. Scope of thesis**

The research presented in this thesis aims to address the development in the synthesis field of crystalline microporous aluminophosphates (AlPO) materials through the interactions between a self-prepared novel imidazolium-based structure-directing agent and precursors of microporous AlPOs. As it is more common for organic molecules such as amines (tetraethylamine, tetrapropylamine) and quaternary amines (tetraethylammonium hydroxide, tetrapropylammonium hydroxide and tetrabutylammonium hydroxide) to be used as structure-directing



agent (SDA) in the hydrothermal synthesis of AlPOs, efforts to produce other alternatives of SDA are also emphasised.

Following the success of imidazoles ([emim]OH and [bmim]OH) in crystallising AlPOs, this research focused on the use of self-designed imidazolium based organic molecule, 3-(2,3-dihydroxylpropyl)-1,2-dimethylimidazolium hydroxide, ([dhpdm]OH), in preparing AlPO materials. At this juncture, different chemical compositions are optimised to hydrothermally synthesise AlPO have been used to investigate the effects of different synthesis parameters such as prolonged heating time, concentration of precursors and SDA on the frameworks structures and morphologies of the crystallised materials. Through an evaluation of the preparation techniques, insight is provided into the candidacy of [dhpdm]OH to participate as a structure- directing agent in the development of versatile AlPO morphologies. This thesis also presented a “greener” approach known as the ionothermal synthesis in the presence of ionic liquid, 1-ethyl-2,3-dimethylimidazolium bromide ([edmim]Br) to crystallise AlPO molecular sieves. Similarly, different synthesis parameters (such as prolonged heating time, concentration of precursors and SDA) were found to have large influences on the frameworks structure and morphologies of the crystallised materials.

Following this introductory chapter, Chapter 2 gives a detailed background on the concepts involving zeolitic materials, structure-directing agents and ionic liquids, hydrothermal and ionothermal syntheses, framework structures and morphologies of crystallised materials. Chapter 3 presents the experimental methodology which includes the preparation of structure-directing agents and synthesis of AlPO materials (both hydrothermal and ionothermal). The characterisation techniques for

organic templates and AlPO materials such as X-ray diffraction analysis (XRD), field emission scanning electron microscopy (FESEM), thermogravimetry and differential thermal analysis (TG/DTA), Fourier transform infrared spectroscopy (FT-IR), nuclear magnetic resonance spectroscopy ( $^{27}\text{Al}$  and  $^{31}\text{P}$  MAS NMR) and nitrogen sorption isotherm analysis are also described in this chapter.

Further to this, the experimental results and discussion are presented in detail in Chapter 4. The findings obtained through ionothermal synthesis using [edmim]Br and hydrothermal synthesis using [dhpdm]OH are discussed at in this chapter. More detailed descriptions which involve the influences of synthesis parameters such as heating time, concentration of precursors and SDA on the crystallisation of AlPOs are also provided in this chapter. Subsequently, two template removal techniques, which are, the conventional calcination method in a muffle furnace, and the microwave-assisted Fenton-liked oxidation process are presented in the later part of Chapter 4. The similarities and differences between these two methods in terms of effectiveness and efficiency in removing the [dhpdm]OH molecules from the micropores of synthesised AlPO are also elaborated. Also, an attempt to use these porous materials in removing methylene blue pollutants is presented in the later part of this chapter.

At the end of this thesis, in Chapter 5, the findings from this study are summarised and the recommendations to future work are proposed in hope to provide a broader insight and prospect in developing the field of microporous zeolitic materials.

## CHAPTER 2

### LITERATURE REVIEW

#### 2.1. Porous materials

Porous material is basically defined as a frame or matrix permeated by an interconnected network of pores filled with a fluid[1]. Generally, there are two types of pores; open pores which connect to the external surface of the material and closed pores which are isolated from the external surface area[2]. These materials with pore sizes near molecular dimensions, such as zeolite and zeotype (aluminophosphate) materials, have become an important class of inorganic crystalline materials with emerging demands of applications[3]. Open porous materials are more favourable amongst catalysis industry and bioreactors while materials with closed pores are commonly used for thermal insulation and low density structural component. Figure 2.1 shows the various classes of nanoporous materials.

According to the International Union of Pure and Applied Chemistry (IUPAC), porous materials are classified according to their pore size[4]. Besides that, porous materials can also be classified based on their framework building blocks such as all-inorganic, hybrid organic-inorganic and all-organic porous polymers and carbonaceous materials[2].

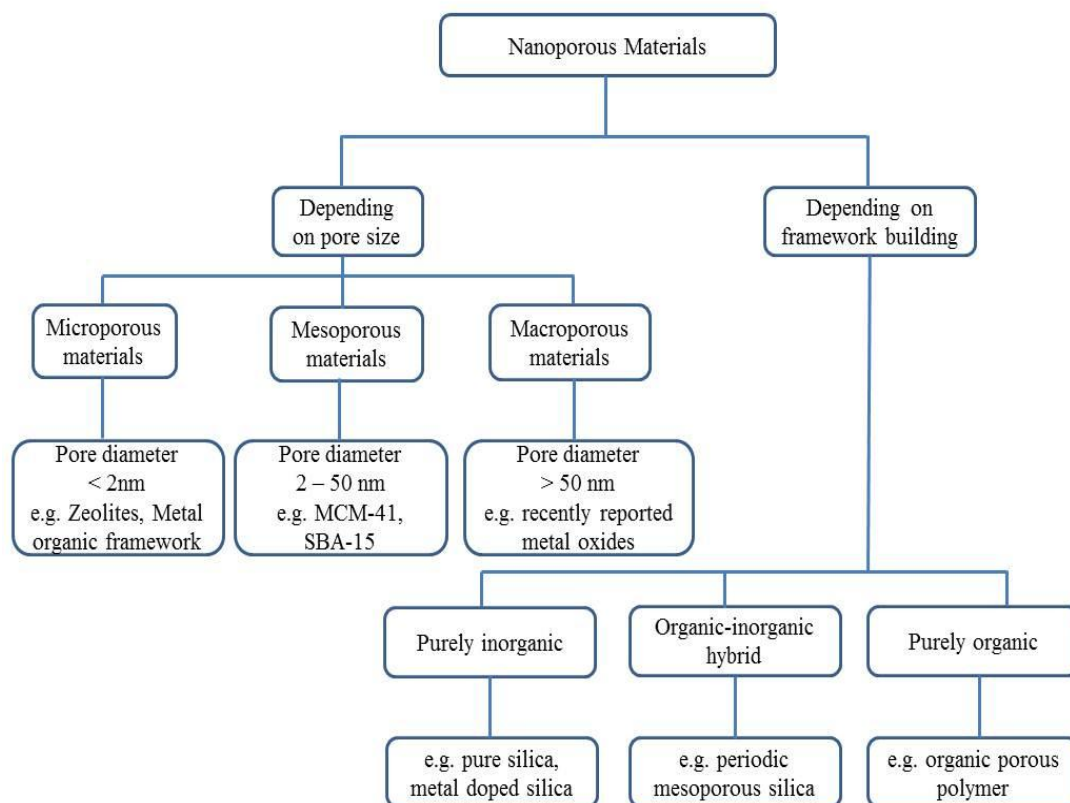


**Figure 2.1.** Schematic representation of the classification of nanoporous materials[2].

### 2.1.1. Microporous materials

Microporous materials which possess a regular network of channels and pores less than about 2 nm are the materials of interest in this thesis. These materials have very low densities and high surface areas which allow them to be applied in adsorption of gases and other small molecules[5]. As these molecular sieves exhibit shape selectivity in which the pores allow certain molecular shapes, sizes or configurations to enter the system, they are widely used in the fields of heterogeneous catalysis and separation[6, 7]. It is known that valences of elements which are stable in a tetrahedral coordination can be located in a microporous framework. This phenomenon is due to the geometric constraints of their bond

lengths and angles[8]. Currently, the most extensively studied groups of microporous materials are the aluminosilicate zeolite and aluminophosphate zeotype materials.

## **2.2. Zeolite and aluminophosphate (AIPO) materials**

### **2.2.1. Zeolite materials**

Derived from the Greek words “zeo” (boil) and “lithos” (stones), zeolite was first discovered about 250 years ago by Alex Fredrik Crönstedt, a Swedish mineralogist, who observed large amount of steam by heating a mineral[9]. The material was later reported to be stilbite[10]. Since then, the science of mineralogy and classification of zeolite minerals have been revolutionised. It was not until 1862 when St Claire Deville claimed to have produced levynite, the first man-made zeolite[11].

However, it was Richard Barrer who reported the first reliable natural zeolite synthesis in the 1940s, earning him the title “The Father of Modern Zeolite Science”[12]. Barrer pioneered a wide range of work pertaining to the microporous sciences: synthesis gel chemistry, diffusion in solid systems, molecular sieves adsorption, etc.[12]. Initially, he focused on investigating the conversion of known mineral phases under the action of strong salt at fairly high temperature (170 – 270 °C) in which two species which exhibit isostructural variants with unique characteristics were obtained[13]. These materials were found to have the KFI structure and led to the synthesis of ZK-5 zeolite[14]. Barrer introduced organic constituents such as alkylamines and alkylammonium salts as space filling agents, structure directing agents and templating agents in the laboratory synthesis of zeolites[15, 16]. Through this finding, it is now possible to create new zeolite frameworks that do not exist in nature.

Generally, zeolites are defined as microporous crystalline aluminosilicates which are constructed from  $\text{AlO}_4$  and  $\text{SiO}_4$  where Al and Si are tetrahedral atoms[17]. These atoms form cages and channels of molecular sieves ranging from about 0.2-1.5 nm in diameter (Figure 2.2a)[10]. Aluminosilicate zeolites have negatively charged framework due to the charge deficiency from  $\text{Al}^{3+}$  in contrast to  $\text{Si}^{4+}$  found in pure silica zeolites. Therefore, charge compensating cations such as  $\text{H}^+$  are required, resulting in the formation of Bronsted acid site on a neighbouring oxygen atom[17].

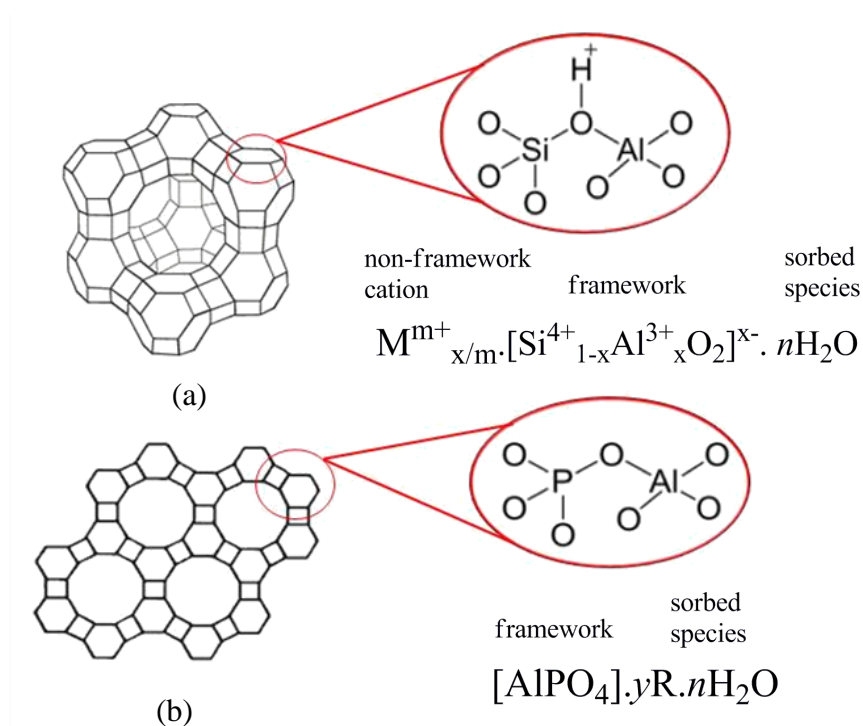


**Figure 2.2.** (a) Zeolite framework with alternating  $\text{AlO}_4^-$  and  $\text{SiO}_4$  tetrahedra and (b) AlPO framework with alternating  $\text{AlO}_4^-$  and  $\text{PO}_4^+$  tetrahedra. R denotes the organic SDA molecule occluded in the pores of AlPO material.

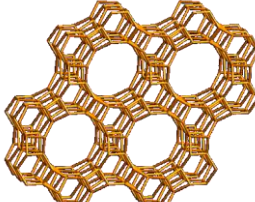
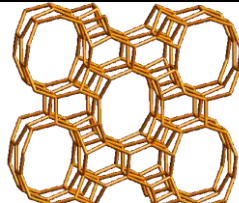
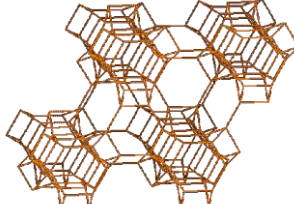
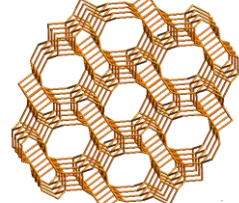
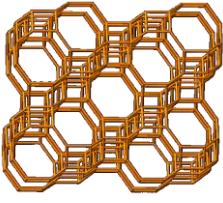
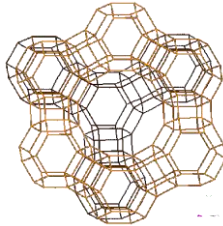
### 2.2.2. AIPO materials

Following the foundation laid by Barrer et al., the next decades witnessed many significant developments extended beyond aluminosilicates. It was in 1982 when Wilson et al. from Union Carbide Corporation discovered microporous crystalline aluminophosphate materials (AIPO), a new family of zeolite-related (zeotype) materials[18]. Elemental substitution of silicon for phosphorus is, ignoring topology, what distinguishes a zeolite from an AIPO. Microporous AIPO materials are not found in nature and their synthesis requires organic template such as organic amine or quaternary ammonium salts which act as structure-directing agents.

The connectivity in AIPOs network is restricted to alternating sequence of Al and P tetrahedral with  $\text{TO}_4$  (with  $\text{T} = \text{Al}$  or  $\text{P}$ ) corner-sharing units which creates cavities and channels of various diameters (Figure 2.2b)[19]. In this manner, the charge neutrality of the AIPO network is ensured as well as prevents the formation of Al-O-Al linkages which are unstable arrangements due to charge repulsion, according to the Lowenstein's rule[20]. Apart from that, P-O-P bridges which are energetically unfavourable, is also not observed in crystalline AIPO[21]. Conceptually, a neutral AIPO framework can be considered to be derived from a neutral silica zeolite by replacement of two  $\text{Si}^{4+}$  cations with one  $\text{Al}^{3+}$  and one  $\text{P}^{5+}$  cation[22].

Today, the AIPO family comprises of more than 50 structures, including 18 analogues of natural or synthetic zeolites[23]. Some of the major structures of AIPO molecular sieves crystallised with different pore sizes are listed in Table 2.1.

**Table 2.1.** Structure frameworks and pore sizes of several AlPO materials[23].

AlPO- <i>n</i>	Structure type	Pore size (Å)	Framework
<i>n</i> = 5	AFI	7.3	
<i>n</i> = 11	AEL	6.0	
<i>n</i> = 17	ERI	4.3	
<i>n</i> = 31	ATO	7.0	
<i>n</i> = 34	CHA	4.3	
<i>n</i> = 37	FAU	8.0	



### 2.2.3. Comparison between zeolite and AIPO materials

Despite zeolites and aluminophosphates are somewhat alike, the chemistry behind the formation of these materials is not similar. Generally, zeolites are formed mostly in alkaline medium (pH 8 ~ 14), where silanol groups may be deprotonated. Synthesis gels with low pH values may lead to the formation of dense phases of aluminosilicates. However, this condition of low acidity or neutral is favoured in the synthesis of aluminophosphates. The synthesis is usually carried out with pH values ranging from 6 to 8[24].

The source of aluminium for both zeolite and AIPO tends to be hydroxides such as aluminium alkoxide or pseudoboehmite. While AIPO relies on orthophosphoric acid as a source of phosphorus, zeolite uses various forms of silica such as fumed silica and colloidal silica. Hence, the precursor gel of AIPO tends to be around neutral and the precursor gel of zeolite is more basic. In addition, the reaction pH is also determined by the template used such as tertiary alkylamine and quaternary ammonium species.

Overall, the framework of zeolite is negatively charged, making it ready for acid catalysis. On the other hand, AIPO framework is neutrally charged and needs to be further modified to display framework catalytic ability by substituting metals such as SAPO and CrAPO[25]. Several other differences between these two materials are summarised in Table 2.2.

**Table 2.2.** Comparison of properties between AlPO and zeolite molecular sieves.

AlPO	Zeolite
Precursor gel contains aluminophosphate.	Precursor gel contains aluminosilicate.
Basic framework elements are Al and P (Figure 2.2b).	Basic framework elements are Si and Al (Figure 2.2a).
Phosphates degrade at low pH to simple structures. The free energy for the hydrolysis of P-O-P bond is relatively favourable.	Silicates and aluminates give a distribution of various sized anions in solution with tendency to larger structures as pH is lowered.
Avoidance of Al-O-Al and P-O-P bonds (Lowenstein's rule) reduces the structural formation to even numbered rings in an alternating form.	Existence of Si-O-Si bonds in aluminosilicate structures make possible formation of even and odd number silicate rings. However, Al-O-Al bond is avoided.

#### 2.2.4. Nomenclature, structure building unit (SBU) and framework structure of AIPO materials

Similar to zeolites, members of the AIPO family are distinguished and named according to protocols set by the Commission of the International Zeolite Association (IZA)[23]. Each AIPO material is designated AIPO- $n$  where  $n$  is a number indicating a specific structure, followed by a three letter framework code. For example, AIPO-5 is assigned the framework code AFI (AIPO Five), ATS (AIPO Thirty-Six) for AIPO-36 and AEL (AIPO Eleven) for AIPO-11. This concept of naming is applied to all aluminophosphates, except those having zeolite analogue such as AIPO-34 (CHA named after zeolite chabazite), AIPO-37 (FAU named after zeolite faujasite) and AIPO-43 (GIS named after zeolite gismondine). As of 2013, there are 206 framework type codes with the major structures and with some of the respective framework of AIPO materials listed in Table 2.1[23].

An AIPO structure can be described in term of building unit (Figure 2.3). Its primary building units (PBU) are composed of tetrahedral  $\text{TO}_4$  units ( $\text{T} = \text{Al}, \text{P}$ ). Each T atom can be described as 4-connected vertices (each T atom is connected to four oxygen atoms) and each oxygen atom is connected to two T atoms. Therefore, the structure of AIPOs can be described as a (4,2)-connected net. The overall AIPO framework structure is based on the secondary building units (SBU) as shown in Figure 2.3[26]. These SBUs are always non-chiral, with the oxygen atoms omitted and represented by the presence of a single straight line between two T atoms (represented by a circle) as illustrated in Figure 2.3. However, the framework composition is restricted to  $\text{Al/P} = 1$ .

The nanocrystalline material of interest in this thesis is the large pore AlPO-5 (AFI) framework as shown in Figure 2.4. Typically AFI framework is described as a one-dimensional channel consisting of a 12-ring pore opening with a diameter of 7.3 Å[27]. The hexagonal structure consists of  $P6cc$  space group. AlPO-5 (AFI) molecular sieve is among the most extensively studied member of the AlPOs due to their use in catalysis, separation, non-linear optics[28, 29]. Up to date, well-defined AFI crystals having various morphologies have been synthesised. For example, Yates et al.[30] reported the synthesis of rod-like AlPO-5 using microemulsions. Additionally, plate-like hexagonal AlPO-5 has been reported by Kornatowski et al.[31] while nanosized AlPO-5 has also been reported by Mintova et al.[32]. The emergence of various morphologies of AlPO-5 crystals is due to the effect of water-soluble organic molecules (commonly referred to as structure-directing agent) under different synthesis conditions.

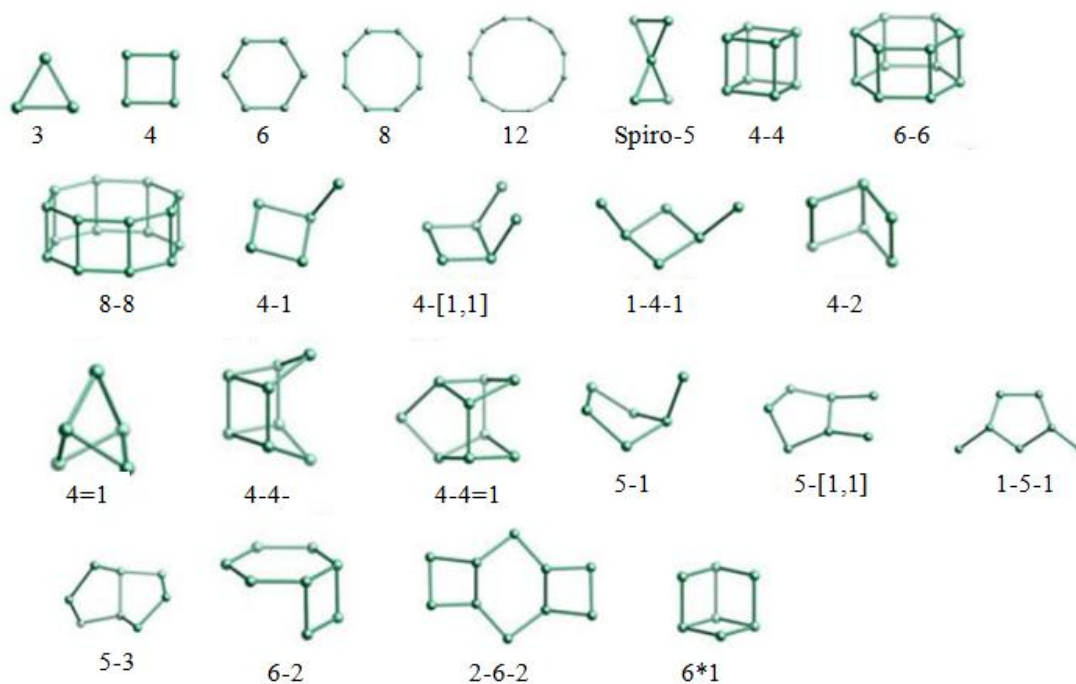


**Figure 2.3.** Secondary building units (SBUs) found in nanoporous materials which contain  $\text{TO}_4$  tetrahedra[13].

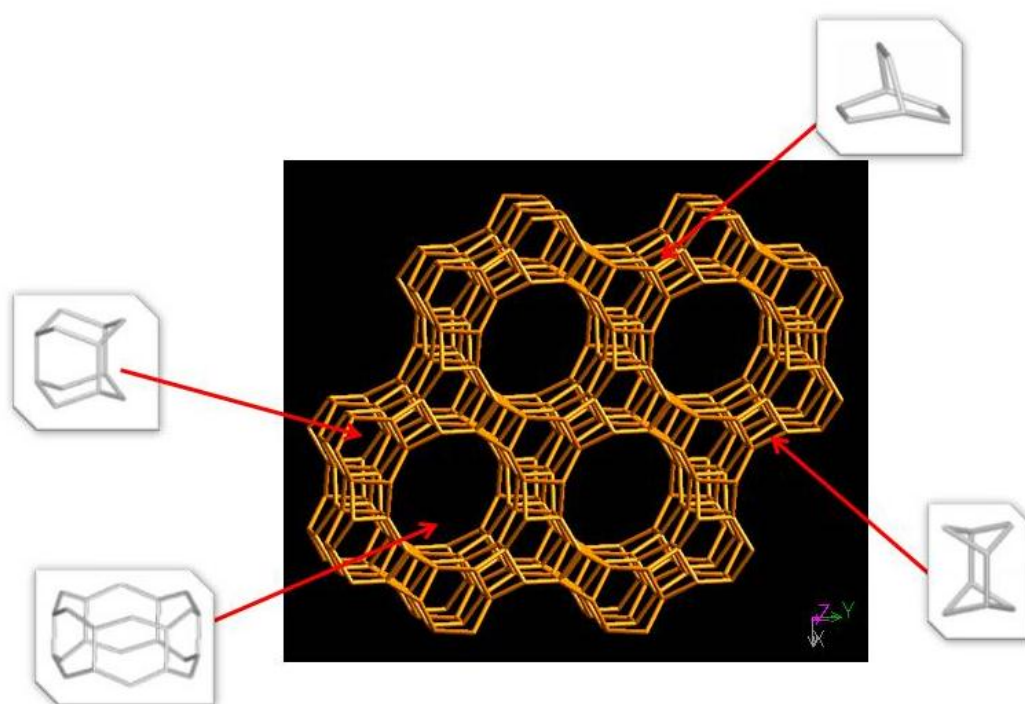


**Figure 2.4.** Illustration of AlPO-5 structure with AFI framework formed by arrangement of separate cages[21].

### 2.3. Hydrothermal synthesis of AlPO materials

Hydrothermal synthesis remains the most common approach in the synthesis of AlPO materials. In this approach, amorphous reactants containing aluminium such as aluminium isopropoxide or aluminium hydroxide hydrate and phosphorus such as orthophosphoric acid are mixed together with water as the solvent and an organic template solution which acts as structure-directing agent in a weakly acidic or weakly alkaline medium ranging from pH 4 to 10. Generally, the chemical composition of a typical reactant gel in the hydrothermal synthesis of AlPOs is expressed in the following form:  $1.0\text{Al}_2\text{O}_3 \cdot x\text{P}_2\text{O}_5 \cdot y\text{R} \cdot z\text{H}_2\text{O}$ , where R is the type organic SDA and  $x$ ,  $y$  and  $z$  represent the molar ratios[22]. The resulted gel mixture is then heated in a sealed autoclave at temperatures between 150 to 250 °C under autogeneous pressure for a specific period of time which could range from hours to days. Subsequently, the amorphous material in the gel mixture will undergo nucleation and crystallisation process (mechanism as described in Section 2.3.2) before the AlPOs crystals are completely formed. The crystals are recovered by filtration for micronsized crystals or centrifugation for nanosized materials, washed thoroughly with water and dried. In order to produce porous AlPOs, the organic cations occluded within the framework are removed. Several methods are proposed for the removal and they are described in Section 2.5.

The type of structure formed by the AlPOs synthesis is dependent on the control of reaction variables such as reactant gel composition and type, time, temperature, pressure, pH, type of organic SDA and history-dependent factors such as ageing, stirring, nature of mixing and order of mixing. It is evidently that changing the molar ratios of reactants used will affect the nature of the final phase formed. Hence, it is difficult to evaluate the effect of varying any one of them as

these variables are dependent of one another. Generally, changing the ratio and content of  $\text{Al}_2\text{O}_3$  and  $\text{P}_2\text{O}_5$  influences the product yield, framework composition and the type of structure formed. Apart from that, the water and hydroxide anion are also considered as contributing factors as they act as gel transport medium. Thus, increasing these concentrations can increase the nucleation and crystallisation rates. The degree of hydrolysis in the system is also determined by water and hydroxide concentrations. For instance, an AIPO material with a chain similar to JDF structure was formed with triethylamine as the organic template, but, increase of water concentrations favoured the formation of AIPO-5 and AIPO-15[33]. In addition, water and hydroxide concentrations also influence the pH of the reactant gel which is essential to successful crystallisation of a molecular sieve, given that aluminophosphates form in weakly acidic or weakly alkaline.

Molecular sieves are usually synthesised at temperatures between 150 to 250 °C under autogeneous pressure. Under these conditions, water has an extremely effective solvating ability which allows for the dissolution and mixing of the solid reagents to form an in homogenous gel, followed by the formation of nucleation centres which subsequently grow to form the crystalline material. Therefore, the synthesis temperature, which affects the self-generated pressure of water, directly influences the crystallisation and structure of the molecular sieve formed[34]. Figure 2.5 shows a typical illustration of the hydrothermal synthesis of AIPO materials.

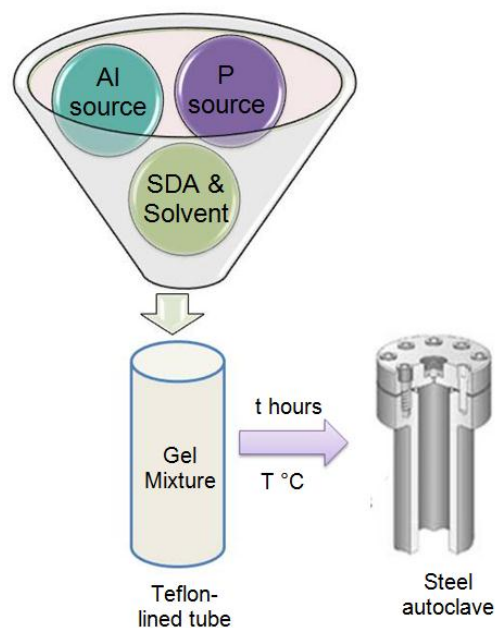


**Figure 2.5.** Schematic illustration of the hydrothermal synthesis of AlPO materials.

### 2.3.1. Structure-directing agent

Structural directing agent (SDA) is an organic additive to facilitate the synthesis of microporous materials such as zeolites and AlPOs[35]. Also known as templates, SDA are organic bases which are included in an inorganic gel medium in which the microporous framework condenses around them. Basically, organic component acts as (a) space filling agents whereby space filling refers to the organic molecules occupying the voids to help stabilise the structure against solvent water which could prevent the growing of the framework, (b) structure directing agent which implies that the SDA is responsible for one unique framework structure, (c) “true” template which occurs when the material adopts the same geometric and electronic configuration as the organic guest[36, 37]. The final structure of the framework reflects, to differing degrees, the shape of the template[38]. Hence, SDA



is a major factor in the crystallisation of molecular sieves as it dictates the size and shape of the pores in these materials.

The structure-directing effect is not as specific as one might expect. In fact, one molecule can direct the crystallisation of several different microporous structures depending on the synthesis conditions. Similarly, one microporous structure can be formed by different SDAs. For example, AlPO-5, which shows the lowest template selectivity, can be formed by at least 20 different organic molecules. Amongst the common SDAs which have successfully produced well-defined AlPO-5 crystals are amines (tetraethylamine, tetrapropylamine), quaternary amines (tetraethylammonium hydroxide, tetrapropylammonium hydroxide, tetrabutylammonium hydroxide) and imidazolium (1-ethyl-2-methylimidazolium hydroxide, 1-butyl-2-methylimidazolium hydroxide)[27, 39, 40]. Despite having the same AFI topology, these materials may possess different structural morphologies such as barrel, rod, spheroidal, hexagonal prism and column shape[27, 31, 40]. It is suggested that the type of SDAs used influences the outcome of the crystallisation[40, 41].

Nevertheless, the nature of the relationship between the structure-directing agent and the AlPO crystalline phase formed is not yet fully understood. It is fundamentally known that the organic supramolecules direct the AlPO framework structures through the organization of the inorganic tetrahedral units into a particular topology, creating the initial blocks for further crystallisation[40]. Therefore, it is still not possible to intentionally synthesise a desired structure of AlPO.

Conceptually, the actual organic-AlPO structure is the outcome of synergistic interactions between the organic cations and the inorganic components that influence the reaction pathway leading to the final outcome of the synthesis[42]. It is believed that the organic SDA influences the synthetic pathways of molecular sieves through

their interactions with the inorganic framework *via* non-covalent bonds. Therefore a suitable candidate of SDA for crystallisation of AIPO molecular sieve should fits several conditions. Among the conditions are, SDA molecules should be stabilised inside the inorganic crystalline phase *via* as many van der Waals interactions as possible. When there is a good geometrical fit in the organic-inorganic composites by van der Waals contacts, the change in the shape of the organic molecules results in different AIPO phases.

Apart from that, it is also reported that SDA should have intermediate hydrophobicity/hydrophilicity when the molecular sieve is synthesised under hydrothermal conditions[43]. Davis et al. proposed a mechanism of assembly involving inorganic-organic composite species whose formation is initiated by overlap of hydrophobic hydration spheres of both the organic and inorganic components with subsequent release of ordered water to establish intermolecular van der Waals interactions[44]. The size and rigidity of SDA also play an important role in providing sufficient room within a particular cage or pore for crystallisation. In terms of flexibility and rigidity, the SDA needs to adopt an optimum conformation in order to be ideally tight to fit in a specific molecular sieve pore. This will then allow long-range stacking sequences for layers of the crystal to grow[42]. In term of size, a bulky molecule of SDA often direct the formation of AIPOs with larger pores due to steric forces[45].

Additionally, the SDA should endure the synthesis conditions, for instance, mild basicity or acidity and high temperature during AIPO synthesis, because decomposed SDA can easily affect the structure of the synthesised product[45].

In short, organic species are found to play a key role during the synthesis of AIPO molecular sieve materials through:

- ❖ Encouraging the formation of nanoporous materials
- ❖ Accessing more metastable states by stabilising the voids of the molecular sieve materials
- ❖ Modifying the Al/P ratio and Al distribution in the gel and in the final product during the formation of AIPO materials
- ❖ Increasing the nucleation and modifying the crystal growth rates.

As such, the study of the template-framework interaction also provides an insight in controlling and synthesising AIPO-5 molecular sieves with different crystal sizes and morphologies[41].

### 2.3.2. Mechanism of crystallisation

The fundamental mechanism of AIPO crystallisation is considered to involve three stages; pre-nucleation, followed by nucleation and finally crystal growth as shown in Figure 2.6.

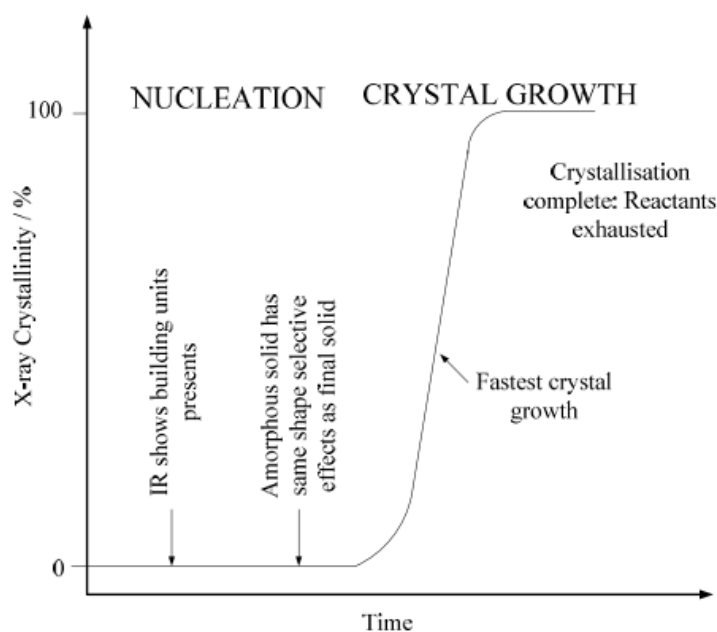


**Figure 2.6.** Process of crystal growth in solution[22].

The initial pre-nucleation stage involves the dissolution and thorough mixing of the starting reagents (Al and P precursors and SDA) by a solvent (usually water) to form an amorphous aluminophosphate layer. The precursor gel is then heated in an oven under autogeneous pressure for a specific period of induction time. During nucleation process, the dissolved particles aggregate and form a nuclei which serves as the crystallisation centre. Following the rapid nucleation process, the nuclei grows larger with time and forms the molecular sieve structures.

Based on this concept, several proposals regarding the crystallisation of AlPO molecular sieves had been surfaced. It has been suggested that direct solid-state transformation occurs to give the final crystalline product. In an alternative approach, Ferey et al. proposed that complete dissolution of the aluminophosphate layer occurs to produce small solution phase building units, which subsequently condensed to form the final crystalline product[46]. Ozin et al. have proposed a model for the formation of AlPO in which two- and three-dimensional structures are formed *via* hydrolysis and condensation of an initial chain structure which forms first in solution[47].

More recently, Grandjean et al. proposed a three stages, one dimensional crystallisation mechanism for hydrothermal synthesis of CoAPO-5 molecular sieves (one of the AlPO framework)[48]. According to Grandjean, the first step of AlPO formation is an initial reaction between Al and P units forming a primary amorphous phase. Moving on to the next step, a progressive condensation of linear Al-O-P chains forms a poorly ordered structure separated by template molecules up to 155 °C. Finally, there is a rapid internal reorganization of the AlPO network leading to crystallisation of the crystal structure. The crystallisation mechanism is illustrated in Figure 2.7.

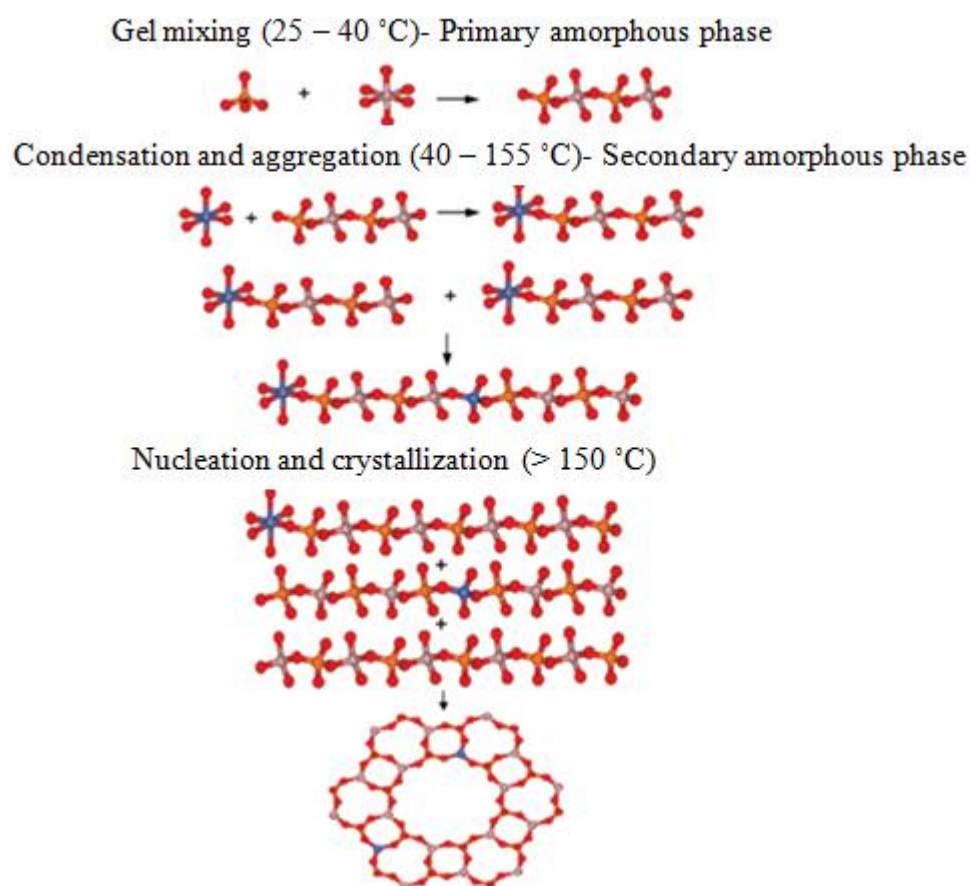


**Figure 2.7.** Schematic representation of the three-stage AlPO-5 crystallisation[43].

Even though the exact mechanism for the formation of zeolite and AlPO molecular sieve materials still remains unclear due to the complexity of the reactions, two other mechanisms are proposed, namely, (i) the solution-mediated transport mechanism, and (ii) the solid hydrogel transformation mechanism. These two mechanisms differ by the presence of liquid component during the crystallisation process.

### 2.3.2.1. Solution-mediated transport mechanism

First reported by Kerr et al., the solution-mediated transport mechanism (Figure 2.8a) involves the dissolution of the aluminosilicate/aluminophosphate gel in the solution phase to form active silicate/phosphate and aluminate ionic species[49]. These ionic species are then transported to the nucleation sites *via* solution-mediated diffusion in which re-crystallisation occurs in the solution to form the structure of the molecular sieve material. Subsequently, crystal growth takes place[50]. A convincing study on this observation was reported by Ueda et al. in which zeolites Y and P were synthesised from a clear solution in the absence of solid phase hydrogel[51]. Similarly, Testa et al. managed to crystallise ZSM-5 and ZSM-11 from clear solution[52].

### 2.3.2.2. Solid hydrogel transformation mechanism

The solid hydrogel transformation mechanism (Figure 2.8b) which was introduced by Breck and Flanigen does not involve the dissolution of the solid gel or the liquid component[17]. This mechanism works in a way that re-organisation of the framework of solid phase aluminosilicate/aluminophosphate hydrogel formed from the condensation of silicate/phosphate and aluminate ions occurs in the early stages of crystallisation. An example of zeolites synthesised *via* this mechanism is the synthesis of ZSM-5 and ZSM-35 by Xu et al.[53]. Xu reported that an amorphous aluminosilicate gel was dehydrated at 550 °C before being treated with liquid triethylamine and ethylenediamine at 160 °C in the absence of water. Since there is no liquid phase silicate/aluminate species present, it was evidently shown that a solid phase transformation had occurred.